Noncanonical sortase-mediated assembly of pilus type 2b in group B *Streptococcus*

Maddalena Lazzarin,* Roberta Cozzi,* Enrico Malito,* Manuele Martinelli,* Mariapina D'Onofrio,† Domenico Maione,* Immaculada Margarit,* and C. Daniela Rinaudo*,[1]

*Novartis Vaccines and Diagnostics, GlaxoSmithKline, Siena, Italy; and †Nuclear Magnetic Resonance Laboratory, Department of Biotechnology, University of Verona, Verona, Italy

ABSTRACT **Group B *Streptococcus* (GBS) expresses 3 structurally distinct pilus types (1, 2a, and 2b) identified as important virulence factors and vaccine targets. These pili are heterotrimeric polymers, covalently assembled on the cell wall by sortase (Srt) enzymes. We investigated the pilus-2b biogenesis mechanism by using a multidisciplinary approach integrating genetic, biochemical, and structural studies to dissect the role of the 2 pilus-2b-associated Srts. We show that only 1 sortase (SrtC1-2b) is responsible for pilus protein polymerization, whereas the second one (Srt2-2b) does not act as a pilin polymerase, but similarly to the housekeeping class A Srt (SrtA), it is involved in cell-wall pilus anchoring by targeting the minor ancillary subunit. Based on its function and sequence features, Srt2-2b does not belong to class C Srts (SrtCs), nor is it a canonical member of any other known family of Srts. We also report the crystal structure of SrtC1-2b at 1.9 Å resolution. The overall fold resembles the typical structure of SrtCs except for the N-terminal lid region that appears in an open conformation displaced from the active site. Our findings reveal that GBS pilus type 2b biogenesis differs significantly from the current model of pilus assembly in gram-positive pathogens.—Lazzarin, M., Cozzi, R., Malito, E., Martinelli, M., D'Onofrio, M., Maione, D., Margarit, I., and Rinaudo, C. D. Noncanonical sortase-mediated assembly of pilus type 2b in group B *Streptococcus*. *FASEB J.* 29, 4629–4640 (2015). www.fasebj.org**

Key Words: crystal structure · backbone protein · ancillary protein · FRET assay

Group B *Streptococcus* (GBS; also referred as *Streptococcus agalactiae*) is a gram-positive human pathogen representing one of the most common causes of life-threatening bacterial infections in neonates and infants. Severe GBS infections can also affect elderly and immunocompromised patients (1). In the past decade, the exponential growth of genome sequence information has led to the identification of covalently polymerized piluslike structures in several gram-positive organisms, including GBS. Pili are protein polymers that form long, thin filamentous structures extending outside of the bacterial cells, mediating adhesion and colonization to host cells, biofilm formation or other activities involved in the virulence and pathogenesis of the bacterium (2). In GBS, pili have been also identified as promising vaccine candidates (3–5). They are composed of many copies of a major protein subunit forming the pilus backbone and of accessory proteins covalently linked *via* transpeptidation reactions catalyzed by specialized sortase (Srt) enzymes, through a common mechanism involving specific motifs and residues present in the pilin subunits (6, 7). These enzymes are membrane-associated cysteine transpeptidases that recognize a conserved carboxylic cell wall sorting signal, consisting of an LPXTG-like sorting motif, where X is any amino acid, followed by a hydrophobic stretch of amino acids and a short, positively charged tail (8). Multiple Srts are often found in the same genome in different bacterial species and can be grouped into different classes and subfamilies based on sequence, membrane topology, genomic localization, and cleavage site preference (9). Gram-positive bacteria express a housekeeping Srt, belonging to class A (SrtA), which is responsible for the cell-wall anchoring of most of the surface proteins (8) and generally use class C sortases (SrtCs) to build multisubunit pili on the cell surface (7). The genes encoding these enzymes are clustered together with the genes encoding their substrates in specific loci of the genome, known as pathogenicity islets. The overall organization of these pilus islands (PIs) is similar among gram-positive bacteria. Genomic analysis has led to the identification in GBS of 3 PIs (PI-1, -2a, and -2b), each coding for at least 2 *srt* genes and 3 pilin subunits harboring an (L/I)PXTG sorting motif (10, 11).

The current model of pilus assembly derives from studies of the archetype sortase-mediated pilus assembly (Spa) A-type pili in *Corynebacterium diphtheriae* and consists of a biphasic process wherein Srt-mediated pilin protein polymerization is followed by a cell wall–anchoring step of the resulting polymer, promoted by the housekeeping Srt (12). Once pilin subunits are synthesized in the bacterial cytoplasm and exported through the general Sec pathway,

Abbreviations: AMS, 4-acetamido-4′-maleimidylstilbene-2,2′-disulfonic acid; AP, ancillary protein; BCA, bicinchoninic acid; BP, backbone protein; ESRF, European Synchrotron Radiation Facility; FRET, fluorescence resonance energy transfer; GBS, group B *Streptococcus*; HMW, high molecular weight; HSQC, heteronuclear single-quantum coherence; IMAC,

(*continued on next page*)

[1] Correspondence: Novartis Vaccines and Diagnostics, Via Fiorentina 1, Siena 53100, Italy, E-mail: daniela.rinaudo@novartis.com

doi: 10.1096/fj.15-272500

This article includes supplemental data. Please visit *http://www.fasebj.org* to obtain this information.

they are retained within the membrane *via* their C-terminal hydrophobic domain and their positively charged tail. Srt enzymes, with their active cysteinyl group, cleave the peptide bond between the threonine (T) and the glycine (G) residues of the LPXTG motif, joining proteins to an amino group located on the next pilin subunit (6, 7). SrtA is generally involved in anchoring of pilus to the cell wall in different species: *C. diphtheriae* (13), *Bacillus cereus* (14), *Streptococcus pneumoniae* (15), and *S. agalactiae* (16, 17).

The assembly and cell wall–anchoring mechanisms of GBS type 1 and 2a pili have been characterized (10, 16, 17), whereas those of pilus type 2b are not yet understood.

In the present work, by combining genetic studies through the generation of mutant GBS strains lacking *srt* genes with biochemical and structural analysis of the corresponding recombinant proteins produced in *Escherichia coli*, we elucidated the roles of the 2 sortases in pilus 2b assembly. The crystal structure of SrtC1-2b described herein enable sequence- and structure-based mutagenesis that, when combined with complementation studies, allowed us to identify the key residues essential for Srt catalytic activity.

MATERIALS AND METHODS

Bioinformatics

SrtC1-2b (CDN66744) and Srt2-2b (CDN66742) sequences were used in the TMHMM Server to predict transmembrane (TM) helices and membrane topology of proteins (Technical University of Denmark, Lyngby, Denmark). Multiple sequence alignments were performed using Mafft and ESPript (18).

Construction of in-frame deletion mutant strains, complementation vectors and site-specific mutagenesis

In-frame deletion knockout (KO) mutant strains were generated by using splicing by overlap extension (SOE) PCR (10). Confirmation of predicted insertions was obtained by PCR amplification and sequencing.

For the generation of complementation vectors pAM_*srtC1*, pAM_*srt2*, and pAM_*ap2*, DNA fragments corresponding to *srtC1*, *srt2*, and *ap2* genes were PCR amplified from GBS strain ABC020017623 genome and cloned into the *E. coli*–streptococcal shuttle vector pAM401/gbs80P+T (10).

Site-directed mutagenesis was performed by the polymerase incomplete primer extension (PIPE) method (19), using the complementation vectors pAM_*srtC1* and pAM_*srt2* as templates for the introduction of specific mutations. The method was improved using HiFi polymerase (Kapa Biosystems, Wilmington, MA, USA) and digesting the DNA template with the *Dpn*I enzyme, to optimize the protocol for large plasmids. Mutations were confirmed by DNA sequencing. All complementation vectors were electroporated into the corresponding KO strains. Complementation was confirmed by checking protein expression by Western blot.

GBS strains and plasmids used are listed in Supplemental Table S1.

GBS protein preparation and immunoblot analysis

GBS strains were grown in Todd Hewitt broth (THB) or chemically defined RPMI-1640 medium at 37°C. For total soluble protein preparation, GBS mid–exponential-phase cells were resuspended in 50 mM Tris-HCl (pH 6.8), containing mutanolysin (Sigma-Aldrich, St. Louis, MO, USA) and complete protease inhibitors (Roche, Basel, Switzerland). The mixtures were then incubated at 37°C for 2 h and the cells lysed by 3 freeze–thaw cycles, and the cellular debris was removed by centrifugation. To visualize proteins released during bacterial growth, supernatants from cultures in RPMI medium were harvested by centrifugation, filtered with a 0.22 μm syringe filter and 10-fold concentrated.

Protein concentration was measured with the bicinchoninic acid (BCA) protein assay (Thermo Scientific-Pierce, Rockford, IL, USA), and equal amounts of proteins were resolved by SDS-PAGE and transferred to nitrocellulose membranes. Membranes were probed with mouse antisera directed against pilus 2b pilin proteins or anti-PcsB as the control (1:1000 dilution), followed by a rabbit anti-mouse horseradish peroxidase–conjugated secondary antibody (Dako, Glostrup, Denmark). Bands were then visualized with an Opti-4CN substrate kit (Bio-Rad, Hercules, CA, USA) or SuperSignal West Pico chemiluminescent substrate (Thermo Scientific-Pierce). Antisera were produced by immunizing CD1 mice with the purified recombinant proteins, as previously reported (5), in compliance with the current Italian legislation (legislative decree 116/92) and the Novartis Animal Welfare Policy and Standards on the Care and Use of Animals in Experimentation. Protocols were approved by the Novartis Animal Ethical Committee (approval number AEC 200825), and authorized by the Italian Ministry of Health (authorization number 21/2009-B).

Cloning, expression, and purification of recombinant proteins

Fragments encoding SrtC1-2b$_{38–245}$ (locus tag GBSCOH1_1278) and Srt2-2b$_{32–199}$ (locus tag GBSCOH1_1276) regions were amplified by PCR from COH1 genomic DNA (accession number HG939456.1) and cloned into the pET15-TEV vector, a modified version of the pET15 vector (Novagen, San Diego, CA, USA), constructed to express N-terminal HIS-tagged (TEV cleavable) proteins by replacing the multiple cloning site of pET15 with a His-TEV-ccdB-chloramphenicol cassette amplified from the SpeedET vector (19). Srt2 cysteine mutants were generated by PIPE site-directed mutagenesis, using as a template the pET15-TEV-Srt2$_{32–199}$ plasmid. A PCR fragment coding the minor ancillary protein 2 of pilus 2b (AP2-2b; locus tag GBSCOH1_1277) was cloned in pET21b(+) vector to produce a C-terminal HIS-tagged protein. The recombinant SrtA was produced as previously reported (17).

Protein expression was performed in *E. coli* Rosetta2 (DE3) cells, by using EnPresso growth systems (BioSilta, Cambridgeshire, United Kingdom) supplemented with 100 μg/ml ampicillin. Bacteria were grown at 30°C for 12 h, and recombinant protein expression was induced by the addition of 1 mM isopropyl β-D-1-thiogalactopyranoside (IPTG) at 25°C for 24 h. The soluble proteins were extracted with CelLytic Express (Sigma-Aldrich) and purified by immobilized metal-affinity chromatography (IMAC) on His-Trap FF-Crude columns (GE Healthcare, Piscataway, NJ, USA). ^{15}N-labeled samples, were eluted with 300 mM imidazole, and the buffer was exchanged with TEV cleavage buffer [50 mM Tris-HCl (pH 8), 1 mM DTT, and 0.5 mM EDTA]

(*continued from previous page*)
immobilized metal-affinity chromatography; IPTG, isopropyl β-D-1-thiogalactopyranoside; KO, knockout; MOLREP, molecular replacement; PDB, Protein Data Bank; PEG, polyethylene glycol; PI, pilus island; PIPE, polymerase incomplete primer extension; rmsd, root-mean-square deviation; SEC, size-exclusion chromatography; SOE, splicing by overlap extension; Spa, sortase-mediated pilus assembly; Srt2-2b, sortase 2 + pilus type 2b; SrtA or C, class A or C sortase; SrtC1-2b, class C sortase 1 + pilus type 2b; THB, Todd Hewitt broth; TM, transmembrane; WT, wild-type

using a PD-10 desalting column (GE Healthcare). The HIS-tag was cleaved by AcTEV protease (12 h at room temperature) and then removed by a subtractive IMAC purification step, followed by size-exclusion chromatography (SEC). The only C-terminal HIS-tagged AP2-2b protein was purified by 1 round of IMAC followed by SEC. The pure protein fractions, which showed a single band by SDS-PAGE, were collected and quantified with the BCA protein assay (Thermo Scientific-Pierce).

For NMR experiments, cells were grown in M9 minimal medium containing 1 g/L of $(^{15}NH_4)_2SO_4$ at 37°C until optical density 600 nm ~0.8 and then protein expression was induced with 1 mM IPTG for 16 h at 25°C. Protein purification was performed with the same protocol reported previously for the unlabeled samples. The proteins were then concentrated by ultrafiltration up to 20 mg/ml.

Crystallization, data collection, and structure determination

Crystallization experiments were performed by the sitting-drop method, mixing 0.2 μl of protein at 30 mg/ml and 0.1 μl of reservoir solutions in 96-well low-profile crystallization plates and using a Crystal Gryphon robot (Art Robbins Instruments, Santa Rosa, CA, USA). Crystals of SrtC1-2b were obtained in condition H2 of the polyethylene glycol (PEG)/ion screen (Hampton Research, Aliso Viejo, CA, USA), containing 0.05 M trisodium citrate (pH 2.3), 16% PEG-3350, 0.05 M Bis-Tris propane (pH 9.7). Before data collection, crystals of SrtC1-2b were first soaked in 10% ethylene glycol as a cryoprotectant and then cooled to 100K in liquid nitrogen.

Diffraction data were measured at 100K on beamline ID29 of the European Synchrotron Radiation Facility (Grenoble, France) and processed with XDS (20) and the CCP4 suite of programs (21). Crystals of SrtC1-2b belong to space group $P2_12_12$, with a calculated Matthews coefficient of 2.3 Å^3/Da, which corresponds to a solvent content of 46%, and 1 molecule of SrtC1-2b occupying the asymmetric unit. The structure of SrtC1-2b was solved by molecular replacement (MOLREP) (22), using coordinates of GBS SrtC1-1 [Protein Data Bank (PDB) ID, 4g1j] as the input template. Structure refinement and rebuilding were performed by Phenix (23) and Coot (24), with final model residual (R) R_{work} and R_{free} statistics of 18 and 22%, respectively. The final refined coordinates of SrtC1-2b include protein residues 39–232, 1 molecule of ethylene glycol, and 90 water molecules. Coordinates and structure factors were deposited in the PDB with accession code 4d7w. Data collection and refinement statistics are summarized in **Table 1**.

TABLE 1. *Data collection and refinement statistics*

Statistic	SrtC1-2b
Wavelength (Å)	1.072
Resolution range	45.92–1.95 (2.02–1.95)
Space group	$P2_12_12$
Unit cell (*a*, *b*, *c*) (Å)	37.5, 124.7, 45.9
Total reflections	56,716 (5190)
Unique reflections	16,211 (1538)
Multiplicity	3.5 (3.4)
Completeness (%)	0.99 (0.96)
Mean $I/\sigma(I)$	15.73 (1.59)
Wilson B-factor (Å^2)	34.81
R_{merge} [a]	0.04989 (0.6619)
R_{meas} [b]	0.0588 (0.7852)
$CC_{1/2}$	0.999 (0.695)
Reflections used in refinement	16,202 (1534)
Reflections used for R_{free}	811 (77)
R_{work} [c]	0.1809 (0.2825)
R_{free} [d]	0.2230 (0.3374)
CC_{work}	0.966 (0.836)
CC_{free}	0.973 (0.614)
Number of nonhydrogen atoms	1645
Macromolecules	1551
Ligands (ethanol)	4
Protein residues	193
RMS (bonds)	0.008
RMS (angles)	1.03
Ramachandran favored (%)	97
Ramachandran allowed (%)	3.1
Ramachandran outliers (%)	0
Rotamer outliers (%)	0.57
Clashscore	3.54
Average B-factor (Å^2)	44.04
Macromolecules	44.08
Ligands (ethanol)	41.29
Solvent	43.47
Number of TLS groups	9

Statistics for the highest-resolution shell are shown in parentheses. [a] $R_{merge} = \Sigma_{hkl}\Sigma_i \mid I_i(hkl) - \langle I(hkl)\rangle \mid / \Sigma_{hkl} \Sigma_i I_i(hkl)$. [b] $R_{meas} = \Sigma_h (n_h/n_h - 1)^{1/2} \Sigma_i \mid \langle I_h\rangle - I_{h,i} \mid / \Sigma_h \Sigma_i I_{h,I}$ where n_h denotes multiplicity. [c] $R_{work} = \Sigma \mid\mid F_{obs}\mid - \mid F_{calc}\mid\mid / \Sigma \mid F_{obs}\mid$. [d] R_{free} = as for R_{work}, but calculated for 5.0% of the total reflections that were chosen at random and omitted from refinement. TLS, translation, libration and screw-rotation parameterization. Ramachandran *Z*-scores and clashscores were determined by MolProbity. (25)

NMR spectroscopy

^{1}H-^{15}N heteronuclear single-quantum coherence (HSQC) spectra were recorded at 25°C on an Avance III spectrometer (Bruker, Karlsruhe, Germany) operating at 600.13 MHz proton Larmor frequency and equipped with a cryogenic probe. A standard ^{1}H-^{15}N HSQC pulse sequence was used, with pulsed field gradients for suppression of the solvent signal and cancellation of artifacts. We acquired 2048 (^{1}H) × 256 (^{15}N) complex data points with spectral windows of 8196.935 Hz (^{1}H) × 2432.718 Hz (^{15}N), 8 transients, and 1.2 s relaxation delay. Processing of all the spectra was performed with Topspin 2.1 (Bruker).

Fluorescence resonance energy transfer assay

The fluorescence resonance energy transfer (FRET) assay was used to monitor the *in vitro* activity of the recombinant Srts by using fluorescently self-quenched peptides, tagged with EDANS as the fluorophore and DABCYL as the quencher, containing the LPXTG-like motif of pilin subunits (**Table 2**). The activity was tested in 300 mM NaCl, 50 mM Tris-HCl (pH 8), 5 or 25 μM Srt enzymes and 32, 64, and 128 μM fluorogenic peptide. The reaction was started by the addition of enzyme and was monitored by measuring the increase in fluorescence every 20 min (λ_{ex} = 336 nm, λ_{em} = 490 nm) at 37°C using an InfiniteM200 spectrophotometer microplate reader (Tecan, Mannedorf, Switzerland). Background measurements were obtained by incubating the fluorogenic peptides at the same reaction conditions, but without Srts.

In vitro cleavage assay

The *in vitro* cleavage assay was performed by mixing 50 μM of the recombinant wild-type (WT) $Srt2_{WT}$ or $SrtA_{WT}$ and 25 μM of the recombinant His-tagged AP2-2b protein in 50 mM Tris-HCl, 300 mM NaCl, 1 mM DTT (pH 8). DTT was added to prevent the formation of potential disulfide bridges leading to aspecific protein dimerization during incubation. As a control, each protein was incubated alone in the same conditions. The incubation was

TABLE 2. *Peptides used in the FRET assay*

Peptide	Sequence
BP-2b = AP1-2b	DABCYL-KGTELPSTGGIGT-EDANS
AP2-2b	DABCYL-QTKGKLPFTGQV-EDANS
AP2-2a	DABCYL-SFLPKTGM-EDANS
AP2-1	DABCYL-RGGLIPKTGEQQ-EDANS

performed at 37°C, and the reaction samples were purified by IMAC and eluted with 300 mM imidazole. Normalized samples by BCA assay were analyzed by Western blot with a serum anti–AP2-2b.

Free cysteines quantification assay

Estimation of free thiols was performed by AMS (4-acetamido-4′-maleimidylstilbene-2,2′-disulfonic acid) to study the involvement of the cysteines' oxidative state in disulphide bond formation (26). AMS has high water solubility and is readily conjugated to free thiols.

Purified recombinant $Srt2_{WT}$ and cysteine mutants were quantified through BCA assay. Half of the samples (reduced form) were incubated with 5 mM DTT for 15 min at 37°C. The buffer was exchanged through PD-10 to remove the DTT, and the resulting proteins were immediately incubated with AMS. The other half of the samples (nonreduced form) was directly incubated with AMS without DTT. Samples (1 ml) of each reaction mixture in 50 mM Tris-HCl, 300 mM NaCl buffer (pH 8.0) containing 25 μM of protein, 250 μM AMS, and 1% SDS were incubated for 30 min at 37°C to complete the reaction. Excess AMS was removed by dialysis.

AMS shows a typical UV absorption at ~328 nm and emission maximum at 408 nm. Fluorescence measurements (λ_{ex} = 322 nm; λ_{em} = 406 nm) were performed to detect the AMS bounded to the free thiols present in the reduced and nonreduced forms of Srt2-2b proteins. A reaction containing AMS and buffer only was performed to measure the background fluorescence.

RESULTS

SrtC1-2b is the only Srt involved in pilus 2b subunit polymerization

Like the other known GBS pilus genomic islands, PI-2b carries 3 genes coding for the structural subunits and 2 genes (*srtC1* and *srt2*) expressing Srt enzymes (**Fig. 1*A***). Gene annotation of the complete genome of GBS COH1 strain, available in the public databases, indicates that the *srtC1* gene encodes the 291-residue-long SrtC1-2b, whereas a second gene (*srt2*) encodes for the shorter putative Srt, the 199-residue-long Srt2-2b. Prediction of TM helices showed that Srt2-2b carries only an N-terminal TM (residues 4–27) and, different from the other GBS pilus-related SrtCs, it lacks the C-terminal TM helix and the region corresponding to the lid loop (Supplemental Fig. S1).

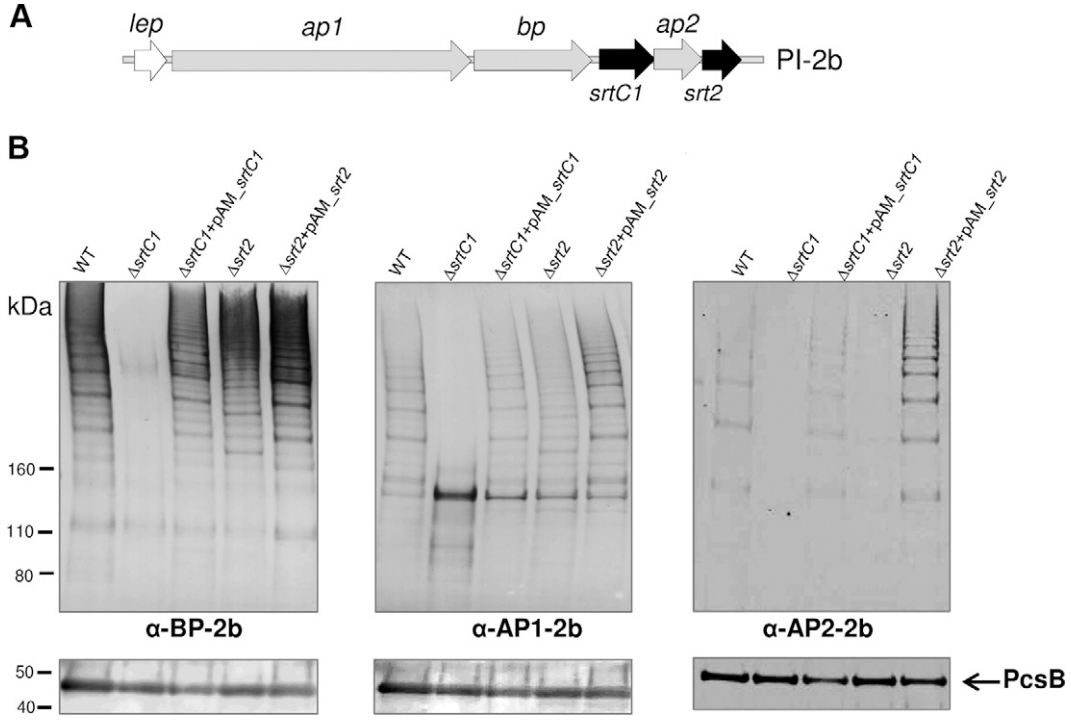

Figure 1. Only SrtC1-2b is essential for polymerizing the pilin proteins into HMW structures. *A*) GBS PI-2b from the GBS COH1 genome. Light gray arrows: genes coding for the structural subunits: backbone protein (*bp*) and ancillary proteins 1 (*ap1*) and 2 (*ap2*). Black: genes coding for the 2 Srts (*srtC1* and *srt2*). A signal peptidase is coded by the *lep* gene (white arrow). *B*) Immunoblot analyses of total proteins prepared from the GBS WT strain and mutant strains lacking the *srtC1-2b* and *srt2-2b* genes (Δ*srtC1* and Δ*srt2*) or mutants complemented by plasmids expressing SrtC1-2b or Srt2-2b (Δ*srtC1*+pAM_*srtC1* and Δ*srt2* +pAM_*srt2*). Nitrocellulose membranes were probed with antisera raised against the backbone protein (α-BP-2b), major ancillary protein (α-AP1-2b), and minor ancillary (α-AP2-2b). Equal loading in each well was verified by probing the same gel with a control antiserum that recognizes the constitutive 47 kDa protein PcsB (bottom; arrow).

To characterize the role of the 2 Srts in pilus-2b assembly, we generated 2 KO mutant strains (Δ*srtC1-2b* and Δ*srt2-2b*) carrying in-frame deletions of each Srt gene in a GBS strain (ABC020017623) containing only the genomic PI-2b. Sequence analysis of PI-2b in this strain confirmed 100% gene conservation with respect to the entire locus sequences of the COH1 strain.

The Δ*srtC1-2b* strain resulted in the deletion of the region corresponding to residues 11–259, whereas the Δ*srt2-2b* mutant resulted in the deletion of Srt2 amino acid residues 14–190.

Total proteins were prepared from each mutant strain and analyzed by SDS-PAGE/immunoblot with antisera specific for each structural subunit (the backbone and the ancillary proteins) (Fig. 1*B*). By this method, covalently linked pili can be detected as a ladder of high-molecular-weight (HMW) bands. As expected, the WT strain revealed the canonical HMW laddering indicative of pilus-like structures whereas, unexpectedly, only the lack of SrtC1 completely abrogated pilus polymerization. Conversely, the Δ*srt2-2b* strain expressed and assembled HMW pili with an efficiency similar to that of the WT strain. Whereas deletion of the *srt2* gene did not affect polymerization of the backbone protein (BP)-2b and the incorporation of the major protein AP1-2b into pili, when anti–AP2-2b antibodies were used, very faint HMW signals were stained and were detectable only after prolonged membrane exposure (Fig. 1*B*). Complementation of the *srtC1* gene restored polymerization to levels comparable to those of the WT strain and complementation of the *srt2* gene into the Δ*srt2-2b* mutant restored pilus staining with anti–AP2-2b. These data clearly indicate that only SrtC1 is involved in BP-2b/AP1-2b polymerization, whereas Srt2-2b appears to be dispensable for pilus 2b formation and could play a role in AP2-2b incorporation into pili or in cell-wall pilus anchoring through the use of the AP2-2b protein.

The lack of Srt2-2b results in release of polymerized pili in the culture supernatant

It is known that the minor ancillary subunit is involved in the cell-wall anchoring of other pili, including GBS pilus type 2a (16, 17), we hypothesized that Srt2-2b, which does not affect the process of pilus protein polymerization, could be involved in pilus anchoring to the cell wall. Moreover, the poor detection of HMW polymers in Δ*srt2-2b* cell-associated proteins with anti–AP2-2b antibodies suggests that the minor subunit AP2-2b is also involved in the anchoring process, possibly as the specific substrate of the Srt2-2b enzyme. To investigate this hypothesis, we analyzed the presence of pili released in the culture supernatant of strains depleted of the *srt2* and *ap2* genes. Thus, we also generated the KO mutant strain (Δ*ap2*) carrying an in-frame deletion of the *ap2* gene. Both mutants were cultured in chemically defined medium, and the amount of pilus polymers present in the extracellular and cell-associated fractions was compared with those produced by WT bacteria.

Proteins from the cell wall and supernatant fractions were extracted, and equal amounts were analyzed by immunoblot with an antiserum specific for the backbone protein. As shown above, in the WT strain, almost all polymerized structures were detectable exclusively in the cell-associated fraction (**Fig. 2**). By contrast, significant amounts of pili were released in the culture supernatants of

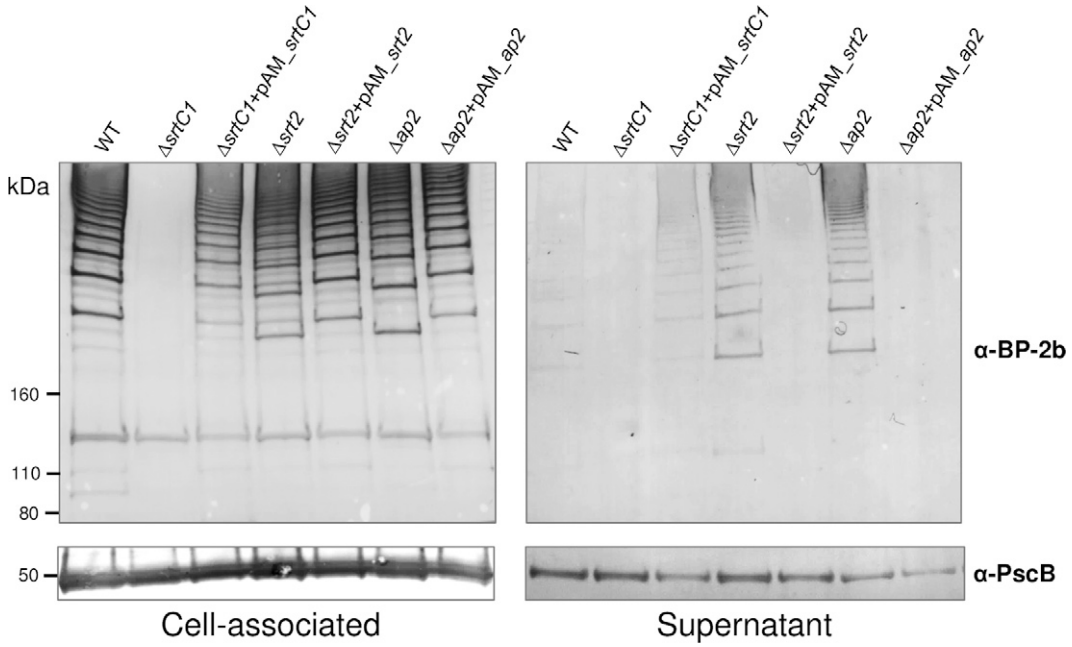

Figure 2. Pili are mostly released in the culture medium of the mutant strains Δ*srt2* and Δ*ap2*. Proteins were collected from RPM1 culture supernatants (right) or extracted from cell pellets (left) of GBS WT or mutant strains depleted of *srtC1*, *srt2* or *ap2* genes (Δ*srtC1*, Δ*srt2*, and Δ*ap2*, respectively) and mutant strains complemented with the plasmids expressing SrtC1, Srt2, or AP2-2b proteins (Δ*srtC1*+pAM_*srtC1*, Δ*srt2*+pAM_*srt2*, and Δ*ap2*+pAM_*ap2*, respectively). Protein fractions were analyzed by immunoblot stained with antibody specific for BP-2b (α-BP-2b, top) and as a quantitative control to ensure equal loading of proteins in each well with the serum against the constitutive protein PcsB (bottom).

Δ*srt2* and Δ*ap2* mutant strains, which revealed comparable phenotypes. Protein profiles similar to those of the WT were restored upon complementation of Δ*srt2* and Δ*ap2* mutants with vectors expressing the corresponding WT genes (Fig. 2). These data support our hypothesis that both Srt2-2b and the minor subunit AP2-2b are involved in cell-wall pilus anchoring.

Srt2-2b specifically recognizes and cleaves the sorting motif of the AP2-2b protein

To further investigate the role of Srt2-2b in pilus 2b assembly, the enzymatic activity of the catalytic domain (residues 32–199) of the recombinant Srt2-2b was assessed *in vitro*. The ^{1}H-^{15}N-HSQC spectrum of the ^{15}N-labeled rSrt2-2b showed a significant dispersion of peaks in both the proton and nitrogen frequency dimensions (spanning ~5 and ~30 ppm, respectively), indicating that the enzyme was correctly folded (data not shown).

To evaluate the Srt2-2b enzymatic activity *in vitro*, we performed a FRET-based assay, using synthetic fluorogenic peptides that mimic the LPXTG-like sorting motif. When the peptide was cleaved by the Srt, the EDANS fluorophore group was separated from the DABCYL quencher group, resulting in an enhanced fluorescence signal. We first tested synthetic peptides carrying the LPXTG-like motifs of the 3 pilus 2b structural proteins (**Table 2**). The LPSTGG-motif of the backbone protein (BP-2b) overlaps with the motif of the major protein AP1-2b and differs from the sorting signal LPFTGQ of the minor protein AP2-2b. A significant increase in the fluorescence signal was observed only when Srt2-2b was incubated with the AP2-2b peptide, indicating that this enzyme specifically recognizes and cleaves this peptide (**Fig. 3*A***). By contrast, the enzyme was not able to cleave either the BP-2b/AP1-2b peptide or the peptide containing the LPKTGM motif of the AP2 of pilus 2a (AP2-2a). We selected this peptide as a control because it is the substrate target of the GBS housekeeping SrtA in the cell-wall anchoring of pilus 2a (17). To confirm the cleavage specificity of Srt2-2b *vs.* the AP2-2b peptide, we verified whether the AP2-2b peptide was also recognized and cleaved by SrtA. Thus, we performed an *in vitro* FRET assay by incubating a purified recombinant SrtA, with the fluorescent AP2-2b peptide or the AP2-2a peptide used as positive control (17). As expected, we observed that the rSrtA enzyme cleaved specifically the AP2-2a peptide, but not the AP2-2b motif, confirming that the AP2-2b protein was the specific substrate of Srt2-2b (Fig. 3*B*).

To further confirm these data we performed an *in vitro* cleavage assay by incubating the Srt2-2b or SrtA enzyme with a recombinant C-terminal His-tagged protein (rAP2-2b) produced in *E. coli*. Srt2-2b or SrtA was incubated at 37°C overnight with rAP2-2b. Reaction mixtures were then purified by IMAC, and the fractions were analyzed by Western blot with the mouse antiserum α-AP2-2b. The IMAC purification allowed elution of only His-tagged proteins or peptides and release in the flow-through fraction of any protein or peptide lacking the His-tag. Accordingly, if the C-terminal His-tagged AP2-2b protein is not cleaved by an Srt at its C-terminal sorting signal, AP2-2b will be collected only in the eluted fraction. By contrast, the cleavage of its sorting signal will be proved by the presence of the cleaved AP2-2b protein in the flow-through fraction. Antibodies specific for the AP2-2b protein revealed a band at a lower molecular mass than the full-length AP2-2b in the flow-through fraction, only when the rAP2-2b protein was incubated with Srt2-2b (Fig. 3*C*), meaning that the protein was cleaved only by Srt2-2b, with the consequent loss of the His-tagged sorting signal. Accordingly, the protein eluted its full length when incubated with the SrtA.

Overall fold of SrtC1-2b

To further elucidate the different roles of SrtC1-2b and Srt2-2b in pilus biogenesis, we performed X-ray crystallography studies. The purified ectodomains of SrtC1-2b (residues 38–245) and Srt2-2b (residues 32–199) were used in crystallization trials. Whereas all attempts to obtain crystals

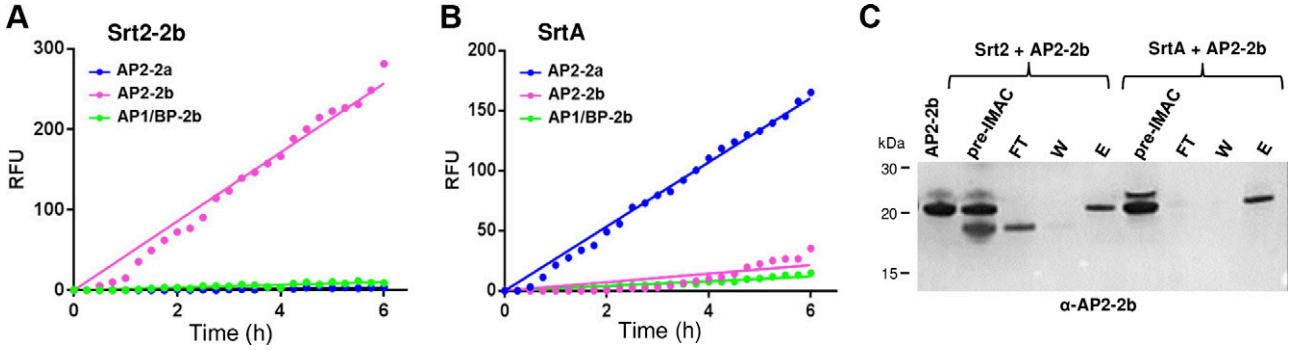

Figure 3. Recombinant Srt2-2b protein cleaves specifically the LPxTG sorting signal of the minor AP2-2b protein. *In vitro* enzymatic activity assessed by FRET analysis of the recombinant WT Srt2-2b (*A*) or SrtA (*B*) proteins using fluorogenic peptides carrying the LPxTG-like motif of minor ancillary AP2-2b, minor ancillary AP2-2a, and the sorting motif of BP-2b overlapping with that of major ancillary AP1-2b (AP1/BP-2b). The fluorescence emission, shown in relative fluorescence units (RFU), was monitored every 20 min. Fluorescence values were normalized against the fluorescence values of the peptide alone. Each assay was performed in triplicate, and the mean values are reported. *C*) *In vitro* cleavage assay of the recombinant C-terminal His-tagged AP2-2b protein incubated either with the recombinant Srt2-2b or SrtA. Cleavage reaction products were then purified by IMAC and the single fractions were analyzed by Western blot with a mouse serum anti–AP2-2b. Fractions in the gel are labeled as FT, IMAC flow-through fraction; W, wash fraction; E, eluted fraction.

of Srt2-2b enzyme failed, the crystal structure of SrtC1-2b was solved at 1.9 Å resolution by molecular replacement in MOLREP (22), starting with a template made of the coordinates of GBS SrtC1-1 (PDB, 4g1j) (**Table 1**).

As for other Srt family members, the overall fold of SrtC1-2b exhibits a core made of a β-barrel compact structure with 10 β strands, surrounded by an α-helical roof composed of 4 consecutive helices (**Fig. 4*A***). The first N-term helix (residues 39–51) runs parallel to the wall of the β-barrel core, whereas the second (residues 53–69), the third (residues 70–75), and the fourth helices (residues 81–90) run almost perpendicular to the first helix and flat on the top of the β-barrel (roof). The loop connecting helices 3 and 4 (residues 76–80) corresponds to the lid region and includes a tryptophan residue (W78). The catalytic triad is made of the residues H149, C211, and R220 that belong to 3 different strands of the lower part of the β-barrel. To confirm the catalytic role of C211 in SrtC1 activity, this cysteine was replaced by site-directed mutagenesis with an alanine into the complementation plasmid pAM_*srtC1*. The generated new plasmid (pAM_$srtC1_{C211A}$) was used to transform the mutant strain Δ*srtC1*. Western blot analysis performed with total protein extracts from the complemented strain (Δ*srtC1*+pAM_$srtC1_{C211A}$) and probed with an anti-backbone protein serum (α-BP-2b) showed that the polymerization of the major subunit of pilus 2b was completely abolished, confirming the catalytic function of C211 (Fig. 4*B*).

Structural comparisons of SrtC1-2b with other Srts

A search of the PDB with the program DALI (27) revealed high structural similarities (*Z*-scores > 2) with more than 100 nonunique Srt family proteins. Thirteen unique entries, corresponding to SrtC or A, were selected among those with the highest *Z*-scores (>13) and lowest rmsd, and these were analyzed by structural superimposition onto the coordinates of SrtC1-2b. This analysis confirmed a highly conserved overall fold, but revealed how the lid of SrtC1-2b assumes an apparent novel conformation. Whereas for most structurally similar entries, the lid is either not visible (likely because flexible and thus disordered), or closed to make interactions with the catalytic triad residues, in SrtC1-2b this assumes an open position. Although DALI also detected as highly similar 2 structures with an open-lid conformation (PDB, 3re9, which is the crystal structure of Srt C1 from *Streptococcus suis*, and PDB, 3tb7, for GBS SrtC1-1 (type I), with *Z*-scores of 23.6 and 22.5, respectively), both these structures have a lid made of a long helix that does not superpose with the lid of SrtC1-2b.

Coordinates of SrtC1 from *S. pneumoniae* (PDB, 2w1j), the only Srt structure with electron density for the whole N-terminal region, and of GBS SrtC1-1 (PDB, 4g1j) were used for further manual structural alignments and analyses, resulting in rmsd values of 1.6 and 1.5 Å, for 2w1j and 4g1j, respectively (**Fig. 5*A*, *B***). Whereas both the β-barrel core and the catalytic triad residues were perfectly superimposed, the lid N-terminal α-helical portion, extending from S74 to D87, revealed a significant difference. The putative regulatory lid tryptophan residue W78 in SrtC1-2b structure, which corresponds to residues W60 and Y92 in 2w1j (Fig. 5*A*) and 4g1j (Fig. 5*B*), respectively, is displaced almost 15 Å away from the catalytic triad in the substrate-binding active site. A multiple sequence alignment of SrtC1-2b and the other crystallized pilus-related Srts showed that only SrtC1-2b does not contain the canonical DPY\W\F lid motif, but only a tryptophan (W78) (**Fig. 6**).

To gain a better understanding of the open lid conformation of SrtC1-2b, we superimposed it onto the coordinates of the open-form structure of the *S. suis* Srt-C1 (PDB, 3re9), obtaining an overall good superimposition (rmsd, 2Å), except for the lid region, where significant differences were again observed (Fig. 5*C*). Upon superimposition of these 2 structures, the regulatory lid Y87 residue of SrtC1_*suis* results positioned farther away from the catalytic triad, as well as from W78 of SrtC1-2b, thus supporting the idea that the lid is an intrinsically highly flexible region (28).

Cys^{115} and Cys^{192} are not essential for Srt2-2b activity *in vivo*

Multiple sequence alignments of Srt2-2b with other GBS Srts revealed the presence of 2 extra cysteines (Cys^{115} and

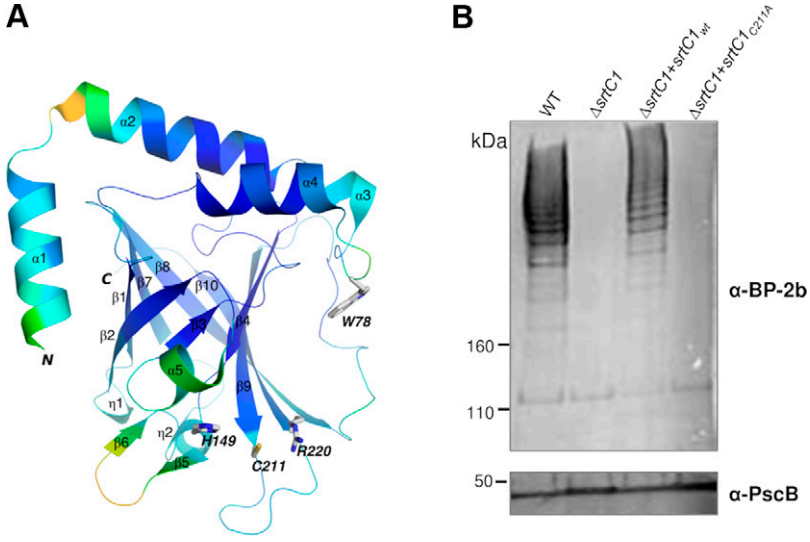

Figure 4. SrtC1-2b crystal structure. *A*) SrtC1-2b is depicted as a graphic colored according to B-factor distribution, using a gradient from blue (22 $Å^2$) to red (120 $Å^2$). Residues forming the catalytic triad and the Trp residue of the lid (W78) are shown with sticks and labeled. *B*) Cys^{211} is responsible for catalytic activity of SrtC1-2b. Immunoblot of total protein extracts from GBS WT, a mutant strain lacking the *srt c1* gene (Δ*srtC1*), and a Δ*srtC1* mutant strain complemented with the plasmid pAM_$srtc1_{WT}$ (Δ*srtC1*+$srtC1_{wt}$) and the plasmid pAM_$srtc1_{C211A}$ (Δ*srtC1*+$srtC1_{C211A}$) expressing the SrtC1 enzyme carrying the substitution of the Cys^{211} with an alanine.

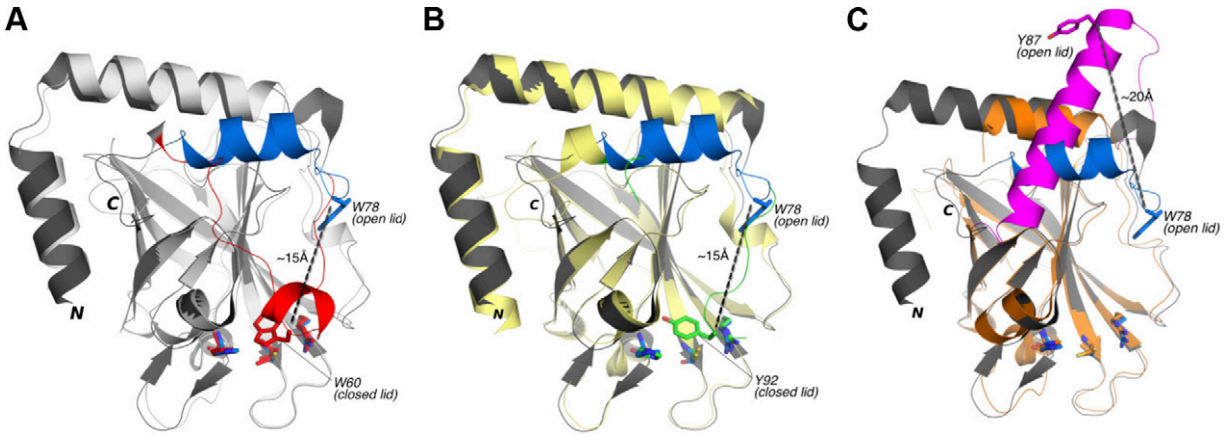

Figure 5. Open and closed lid of SrtC structures. Superimposition of GBS SrtC1-2b (PDB, 4d7w) onto the structure of SrtC1 of *S. pneumoniae* (PDB, 2w1j, light gray) (*A*), onto the structure of GBS SrtC1-1 from pilus type 1 (PDB, 4g1j, light yellow) (*B*), and onto the SrtC1 from *S. suis* (PDB, 3re9, orange) (*C*). Dark gray: the structure of SrtC1-2b. The lid regions of 4d7w, 2w1j, 4g1j, and 3re9 are blue, red, green, and magenta, respectively. Superimposed residues of the catalytic triads of all structures, as well as aromatic residues of the lids, are shown with sticks and colored according to the structure or region to which they belong. The distance between Cα atoms of the aromatic lid residues is also shown, to highlight the displacement of the lid in SrtC1-2b.

Cys^{192}) in addition to the one that is part of the conserved canonical triad (made of H117, C180, and R187). Moreover, Srt2-2b does not contain the canonical DPY\W\F lid motif either, showing even a large deletion in this region compared with other Srts (Supplemental Fig. S1). To investigate the possible involvement of those cysteines in the catalytic activity of Srt2-2b, we generated complementation vectors expressing 3 mutant enzymes (pAM_*srt2*$_{C115A}$, pAM_*srt2*$_{C180A}$, and pAM_*srt2*$_{C192A}$). After complementation of the Δ*srt2* mutant strain, the effect of each mutation was analyzed by Western blot, checking the release of polymerized HMW structures in the culture medium supernatants from complemented strains. As expected, no HMW polymerized structures were found in the medium supernatants of the complemented strains expressing the WT and the mutated $Srt2_{C115A}$ and $Srt2_{C192A}$ enzymes (**Fig. 7*A***). By contrast, by complementing the KO Δ*srt2* strain with the plasmid expressing the Srt carrying the C180A, the substitution-released polymerized pili were still detected in the culture medium, revealing that C180 is the catalytic residue essential for Srt2 activity.

Srt2-2b is reversibly inactivated by oxidation

To better investigate the contribution of the cysteines in Srt2-2b to the *in vitro* enzymatic activity of Srt2 mutants ($Srt2_{C115A}$, $Srt2_{C180A}$, and $Srt2_{C192A}$) was assessed by FRET assay, and the presence of free thiols by AMS assay, checking as a prerequisite that the mutations C115A and C192A did not affect the general fold of the mutant enzymes. The HSQC spectra of the ^{15}N-labeled $Srt2_{C115A}$, and $Srt2_{C192A}$ mutants showed signal dispersions comparable to those of the WT protein, meaning that each single mutation did not alter the overall structure of the proteins, and the native enzyme fold was preserved (Fig. 7*B*).

For FRET experiments, Srt2-2b mutants were incubated with different concentrations of the fluorescent AP2-2b peptide. In agreement with the data above, the activity of the $Srt2_{C180A}$ enzyme was completely abolished, further confirming the catalytic role of this residue. The mutant $Srt2_{C192A}$ showed an enhanced cleavage activity compared with that of the WT enzyme, whereas the mutant $Srt2_{C115A}$ revealed highly reduced activity (Fig. 7*C*). With the exception of the C180 mutant, the activity of the other 3 samples correlated with the fluorescence values in the AMS assay (Fig. 7*D*). AMS specifically binds to free thiols and the sample fluorescence measured after the removal of AMS excess is directly proportional to the number of free cysteines (25). In fact, the $Srt2_{C192A}$ mutant that showed maximum cleavage activity revealed also the higher AMS fluorescence. Pretreatment of this protein with DTT did not modify the fluorescence value, meaning that the number of its free cysteines does not change in the reduced form; the catalytic Cys^{180} remains free and thus active. On the contrary, the $Srt2_{C115A}$ mutant characterized by low FRET activity showed in absence of DTT at low AMS fluorescence that increased when the sample was pretreated with DTT. This observation suggests that the low enzymatic activity *in vitro* of $Srt2_{C115A}$ is due to a disulfide bond formation between Cys^{192} and the catalytic Cys^{180}, which thus locks in its activity. As $Srt2_{WT}$ showed an intermediate enzymatic activity and intermediate AMS fluorescence value, a balance between the Cys^{192}–Cys^{180} and Cys^{192}–Cys^{115} disulfide bonds could exist. AMS results suggest that in $Srt2_{WT}$ Cys^{192} could be engaged in a disulfide bond with either Cys^{115} or Cys^{180}, since both the mutants $Srt2_{C115A}$ and $Srt2_{C180A}$ after incubation with AMS yielded in the same fluorescence values. On the contrary, Cys^{115} and Cys^{180} did not interact directly with each other in a disulfide bond, and indeed, the mutant $Srt2_{C192A}$ seemed to contain free cysteines in all tested conditions (Fig. 7*D*).

DISCUSSION

In this work, we explored the biogenesis mechanism of GBS pilus type 2b by dissecting the specific role of the 2 pilus-associated Srts. The most significant finding is that pilus 2b polymerization and cell-wall anchoring

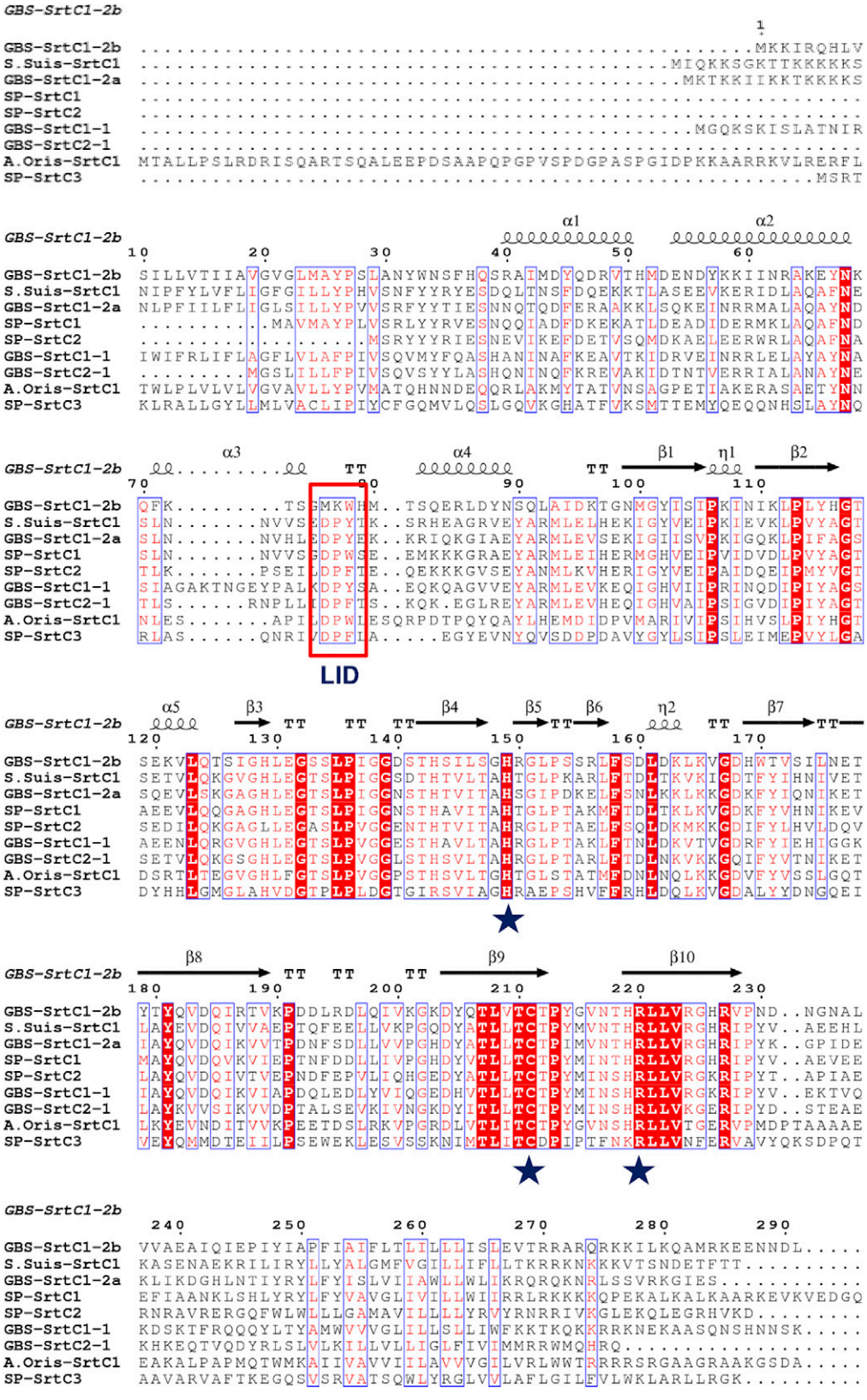

Figure 6. Multiple sequence alignment of the pilus-forming Srts deposited in the PDB. Structure-based sequence alignment by ESPript of GBS SrtC1-2b (PDB, 4d7w); GBS pilus 1 SrtC1-1 (PDB, 4g1j) and SrtC2-1 (PDB, 4h1h); GBS pilus 2a SrtC1-2a (PDB, 3o0p); *S. pneumoniae* Srt C1 (PDB, 2w1j); SrtC2 (PDB, 3g69) and SrtC3 (PDB, 2w1k); and *S. suis* (PDB, 3re9) and *Actinomyces oris* (PDB, 2xwg) SrtC1. Red background: identical residues; red residues in blue boxes: similar residues. Blue stars: residues located within the active site cleft (His, Cys, and Arg) and conserved among all Srts; red box: lid residues DPF\Y\W.

mechanisms appear to be noncanonical, differing significantly from the current model of gram-positive pilus assembly, where pilin subunit polymerization is catalyzed by class C Srts, and the housekeeping SrtA catalyzes pilus anchoring to the cell wall (6, 8). The other 2 pilus types (1 and 2a) expressed in GBS follow this canonical assembly model, where 2 SrtCs act redundantly as pilin polymerases, and pilus cell-wall anchoring is completed by SrtA (10, 11, 16, 17). By contrast, pilus 2b subunits appeared to be polymerized exclusively by 1 Srt (SrtC1-2b), because only the

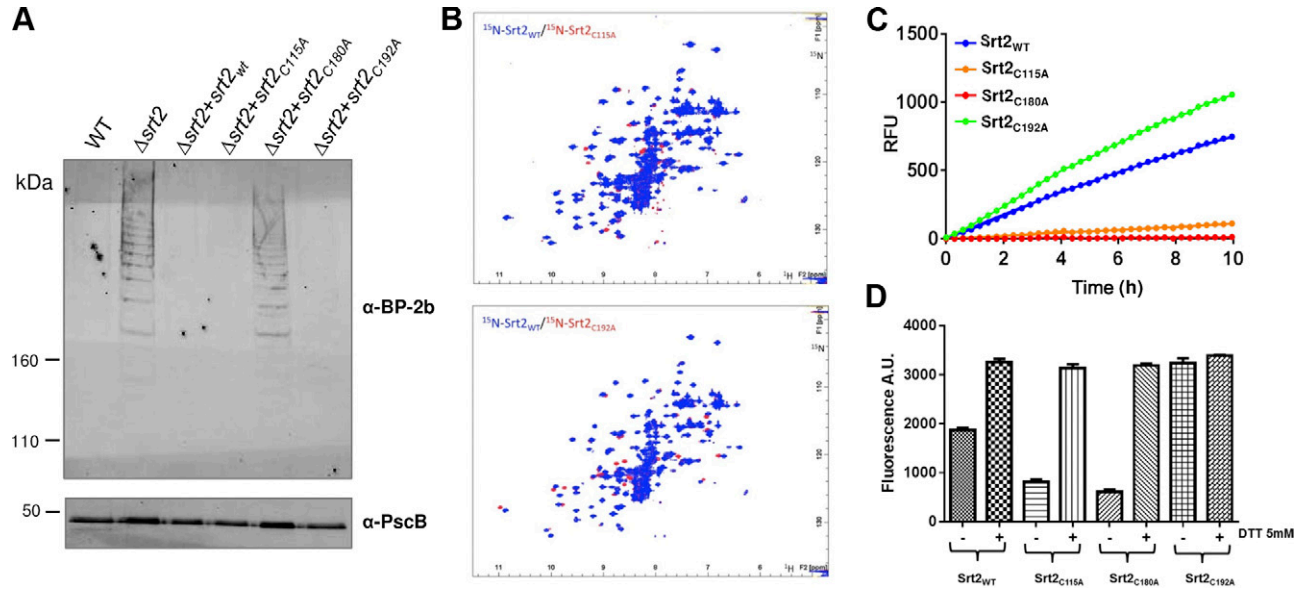

Figure 7. Srt2-2b mutant protein characterization. *A*) Cys^{180} is responsible for catalytic activity of Srt2-2b. Western blot analysis of total proteins collected from culture medium supernatants of the GBS WT strain, GBS-KO strain depleted of the *srt2* gene (Δ*srt2*) and Δ*srt2* strain complemented with the plasmids pAM_$srt2_{WT}$ (Δ*srt2*+$srt2_{wt}$), pAM_$srt2_{C115A}$ (Δ*srt2*+$srt2_{C115A}$), pAM_$srt2_{C180A}$ (Δ*srt2* +$srt2_{C180A}$), and pAM_$srt2_{C192A}$ (Δ*srt2*+$srt2_{C192A}$), expressing Srt2 cysteine mutant enzymes. Nitrocellulose membrane was probed with a mouse antiserum raised against BP-2b (α-BP-2b). Equal loading in each well was verified by probing the same gel with a control antiserum specific for the constitutive 47-kDa PcsB protein (bottom). *B*) Superimposition of NMR ^{1}H-^{15}N HSQC spectra of the purified ^{15}N-labeled $Srt2_{C115A}$ and ^{15}N-$Srt2_{C192A}$ mutants (red) on HSQC spectra of the ^{15}N-$Srt2_{WT}$ (cyan). *C*) FRET assay of the recombinant SrtC2 WT and cysteine mutants (5 μM) incubated with 128 μM of the fluorescent peptide carrying the AP2-2b LPXTG motif. The values of triplicate samples, recorded every 20 min as relative fluorescence units (RFU), are reported. *D*) Free cysteines quantification by AMS assay. AMS binding to free cysteine thiols was revealed by the fluorescence measurement.

deletion of the *srtC1-2b* gene totally abrogated protein polymerization, whereas the KO strain that did not express the second Srt (Srt2-2b) was able to produce HMW pilus polymers similarly to the WT strain. However, the polymers were released into the culture supernatant, a phenotype observed also when bacterial cells lacked the minor ancillary protein AP2-2b. The data are in line with the involvement of Srt2-2b in pilus cell-wall anchoring and of the minor AP2-2b subunit as anchor protein. Accordingly, *in vitro* experiments performed to assess the cleavage activity of a recombinant Srt2-2b enzyme showed that the protein recognized and hydrolyzed only the sorting signal of AP2-2b, whereas it did not cleave the sorting motif of BP-2b or AP1-2b, further confirming that the enzyme does not act as a pilin polymerase. The minor AP2-2b subunit was not recognized by the housekeeping SrtA, as is the case during cell-wall anchoring of pili in most gram-positive bacteria (9, 13–17). Therefore, although the 3 GBS pili appeared to be highly similar both structurally and at the level of gene organization of their genomic PIs, only pilus type 2b seemed to follow a unique assembly mechanism. Cell-wall attachment of Spa-type pili in *C. diphtheriae* is mediated by a housekeeping Srt, SrtF. Nevertheless, when this Srt is absent, an SrtC that is normally responsible for pilin polymerization can be activated to catalyze the pilus anchoring step, although less efficiently than SrtF (29). In *Bacillus anthracis* and *Streptococcus pyogenes*, under specific environmental conditions, SrtBs or SrtDs can be activated for targeting proteins to the cell wall in competition with the constitutive SrtA (8, 30, 31). These data highlight the universality of the transpeptidation mechanism catalyzed by all Srt family members and their redundancy and surprising promiscuity in the substrate recognition.

To better understand the distinct roles of the 2 pilus 2b Srts in pilus assembly, we compared these Srts with other well-characterized gram-positive pilus-related Srts both at the sequence and structural level. Beyond the very low percentage of amino acid identity observed (32), the most significant peculiarity shared by the 2 pilus 2b enzymes was the lack of the conserved DPY\W\F residues in the N-terminal lid region, currently considered a characteristic feature of all pilus-specific Srts (28, 33). This highly flexible lid loop, which confers thermodynamic and proteolytic stability to the enzymes, has an important role in Srt activation, specifically in the regulation of substrate accessibility to the active site (32–36). In SrtC1-2a it has been recently demonstrated that a single residue in the DPY\W\F motif can abolish the enzyme catalytic activity by interacting with the catalytic cysteine. The enzyme activity can then be induced through a displacement of the lid from the enzyme active site, probably as a result of the interaction with the substrate protein and other unknown factors (37). The crystal structure of SrtC1-2b revealed excellent electron densities for the entire N-terminal α-helical roof surrounding the conserved β-barrel core and including residues S74–D87 of the putative lid region. On the contrary, other Srt structures often lacked electron densities in the lid region. This observation suggests that the lid positioned as in the conformation observed in the structure of SrtC1-2b has an increased stability, as also supported by the B-factor values of the fragment of residues 76–92, with a value of 38 $Å^2$ *vs.* the overall average of 44 $Å^2$. Moreover,

this loop is found far away from the active site in the β-barrel core and does not cover the substrate binding groove, thus resulting in a wide-open state. This observation suggests a possible different mechanism by which the substrate can gain access to the catalytic core. However, analyses of the crystal contacts in front of the lid do not allow us to exclude a contribution to the currently observed lid configuration by symmetry-related molecules of this particular crystal form of SrtC1-2b, which shows a tight packing incompatible with a closed configuration (as seen for example for SrtC1 of *S. pneumoniae*, PDB, 2w1j).

Superimposition of SrtC1-2b structure onto the open-form structure of Srt C1 from *S. suis* (38) (Fig. 5*D*) indicated that *S. suis* SrtC1 is in an even more open conformation than SrtC1-2b. From these observations, we could speculate that the lid region is capable of exploring wide conformational space, going from a wide-open state (an *S. suis* SrtC1-like conformation) to a closed state (an *S. pneumoniae* SrtC1-like or GBS SrtC1-1-like conformation), through an open-intermediate state, as observed in the SrtC1-2b structure. However, because the SrtC1-2b structure is in an open conformation, the role of the putative lid residue W78 in enzyme regulation must be demonstrated.

Having failed to obtain crystals of Srt2-2b protein, sequence analysis revealed significant differences compared with the other pilus-related Srts, including those of GBS (Supplemental Fig. S1). The N terminus is significantly shorter, and the lid region, as well as the C-terminal TM helix, is totally missing. These regions have been considered SrtC-typical elements that are required for an efficient pilin protein polymerization (19).

Based on the current Srt classification reported by Spirig *et al.* (9), a multiple sequence alignment of pilus 2b SrtC1 and Srt2 protein sequences with a selected set of proteins belonging to the 6 classes of Srts from gram-positive bacteria, confirmed that SrtC1-2b clusters with the clade of SrtCs, in agreement with its function of pilin polymerase. By contrast, Srt2-2b is clearly out of the SrtC cluster, apparently more phylogenetically close to SrtAs (but certainly not a canonical SrtA), accordingly with its role just in pilus 2b anchoring to the cell wall, but not in pilus protein polymerization (Supplemental Fig. S2). These observations, predicted by the genomic annotation, enable us to state that, despite sequence and structural differences, SrtC1-2b is a typical SrtC, whereas Srt2-2b is not a SrtC and cannot be partitioned into 1 of the 6 distinct families of Srts.

The presence in Srt2-2b of 2 additional cysteine residues, potentially able to form a disulfide bond with the catalytic Cys^{180} and thus inactivating the enzyme, led us to speculate that the activation of Srt2-2b could be controlled by a redox regulation mechanism, alternative to the lid displacing mechanism. This hypothesis is also supported by our observations from the AMS and FRET assays. Several other extracellular or membrane-associated enzymes have already been shown to be subject to oxidative inactivation *via* disulfide bond formation (39, 40). This mechanism presumably serves as a redox switch to regulate the enzyme activity in extracellular environments that are generally characterized by oxidative conditions where disulfide bonds formation is favored (41).

Another aspect of Srt activity regulation *in vivo* takes into account the involvement of chaperone-like proteins in pilus assembly. An example is pilus polymerization in *S. pyogenes*, where gene knockout studies showed that the Srt Spy0129 is not sufficient alone to polymerize the backbone protein Spy0128, but the signal peptidase-like protein SipA, encoded in the same genomic pilus operon, is also necessary for polymer formation (42). The need for a peptidase-like protein chaperone for pilus assembly *in vivo* may be a common theme in the regulation of pilus Srt activity. Other pilus gene clusters containing genes encoding peptidase-like proteins can be found in *Actinomyces naeslundii* (43), *S. pneumoniae* (44), and *S. suis* (45) and, in GBS, the genomic PI-2b contains a gene coding for a LepA-type signaling peptidase as well. Further efforts are needed to understand the role of this protein in PI-2b assembly, as well as how potential different Srt activation pathways, likely involving unknown genes, affect the ability of GBS strains that express different pilus types to adapt to different environmental conditions.

In conclusion, Srt enzymes have a critical role in gram-positive bacteria, because of their function to covalently link to the cell wall surface proteins or pilus polymers that have been associated with bacterial virulence and pathogenesis. Furthermore, GBS pilin subunits are highly immunogenic vaccine targets, and most of the epidemiologically relevant GBS clinical isolates express at least 1 pilus type. PI-2b has been associated with a hypervirulent clone (ST17-serotype III) that is responsible for most neonatal invasive diseases (4), but it remains uncharacterized so far. Thus, fully understanding the molecular basis of the mechanism of pilus biogenesis at the membrane environment during the establishment and persistence of infections by gram-positive microorganisms remains of great scientific interest. FJ

The authors thank R. Rosini and E. Campisi (Novartis Vaccines and Diagnostics, GlaxoSmithKline) for critical and useful discussion. This work was supported by the Joint Research Project 2010 between the University of Verona and Novartis Vaccines and Diagnostics.

REFERENCES

1. Le Doare, K., and Heath, P. T. (2013) An overview of global GBS epidemiology. *Vaccine* **31** (Suppl 4), D7–D12
2. Mandlik, A., Swierczynski, A., Das, A., and Ton-That, H. (2008) Pili in Gram-positive bacteria: assembly, involvement in colonization and biofilm development. *Trends Microbiol.* **16**, 33–40
3. Maione, D., Margarit, I., Rinaudo, C. D., Masignani, V., Mora, M., Scarselli, M., Tettelin, H., Brettoni, C., Iacobini, E. T., Rosini, R., D'Agostino, N., Miorin, L., Buccato, S., Mariani, M., Galli, G., Nogarotto, R., Nardi-Dei, V., Vegni, F., Fraser, C., Mancuso, G., Teti, G., Madoff, L. C., Paoletti, L. C., Rappuoli, R., Kasper, D. L., Telford, J. L., and Grandi, G. (2005) Identification of a universal Group B streptococcus vaccine by multiple genome screen. *Science* **309**, 148–150
4. Margarit, I., Rinaudo, C. D., Galeotti, C. L., Maione, D., Ghezzo, C., Buttazzoni, E., Rosini, R., Runci, Y., Mora, M., Buccato, S., Pagani, M., Tresoldi, E., Berardi, A., Creti, R., Baker, C. J., Telford, J. L., and Grandi, G. (2009) Preventing bacterial infections with pilus-based vaccines: the group B streptococcus paradigm. *J. Infect. Dis.* **199**, 108–115
5. Nuccitelli, A., Cozzi, R., Gourlay, L. J., Donnarumma, D., Necchi, F., Norais, N., Telford, J. L., Rappuoli, R., Bolognesi, M., Maione, D., Grandi, G., and Rinaudo, C. D. (2011) Structure-based approach to rationally design a chimeric protein for an effective vaccine against Group B *Streptococcus* infections. *Proc. Natl. Acad. Sci. USA* **108**, 10278–10283
6. Kang, H. J., and Baker, E. N. (2012) Structure and assembly of Gram-positive bacterial pili: unique covalent polymers. *Curr. Opin. Struct. Biol.* **22**, 200–207

7. Hendrickx, A. P., Budzik, J. M., Oh, S. Y., and Schneewind, O. (2011) Architects at the bacterial surface: sortases and the assembly of pili with isopeptide bonds. *Nat. Rev. Microbiol.* **9**, 166–176
8. Schneewind, O., and Missiakas, D. (2014) Sec-secretion and sortase-mediated anchoring of proteins in Gram-positive bacteria. *Biochim. Biophys. Acta* **1843**, 1687–1697
9. Spirig, T., Weiner, E. M., and Clubb, R. T. (2011) Sortase enzymes in Gram-positive bacteria. *Mol. Microbiol.* **82**, 1044–1059
10. Rosini, R., Rinaudo, C. D., Soriani, M., Lauer, P., Mora, M., Maione, D., Taddei, A., Santi, I., Ghezzo, C., Brettoni, C., Buccato, S., Margarit, I., Grandi, G., and Telford, J. L. (2006) Identification of novel genomic islands coding for antigenic pilus-like structures in *Streptococcus agalactiae*. *Mol. Microbiol.* **61**, 126–141
11. Dramsi, S., Caliot, E., Bonne, I., Guadagnini, S., Prévost, M. C., Kojadinovic, M., Lalioui, L., Poyart, C., and Trieu-Cuot, P. (2006) Assembly and role of pili in group B streptococci. *Mol. Microbiol.* **60**, 1401–1413
12. Ton-That, H., and Schneewind, O. (2003) Assembly of pili on the surface of *Corynebacterium diphtheriae*. *Mol. Microbiol.* **50**, 1429–1438
13. Mandlik, A., Das, A., and Ton-That, H. (2008) The molecular switch that activates the cell wall anchoring step of pilus assembly in gram-positive bacteria. *Proc. Natl. Acad. Sci. USA* **105**, 14147–14152
14. Budzik, J. M., Marraffini, L. A., Souda, P., Whitelegge, J. P., Faull, K. F., and Schneewind, O. (2008) Amide bonds assemble pili on the surface of bacilli. *Proc. Natl. Acad. Sci. USA* **105**, 10215–10220
15. Shaik, M. M., Maccagni, A., Tourcier, G., Di Guilmi, A. M., and Dessen, A. (2014) Structural basis of pilus anchoring by the ancillary pilin RrgC of *Streptococcus pneumoniae*. *J. Biol. Chem.* **289**, 16988–16997
16. Nobbs, A. H., Rosini, R., Rinaudo, C. D., Maione, D., Grandi, G., and Telford, J. L. (2008) Sortase A utilizes an ancillary protein anchor for efficient cell wall anchoring of pili in *Streptococcus agalactiae*. *Infect. Immun.* **76**, 3550–3560
17. Necchi, F., Nardi-Dei, V., Biagini, M., Assfalg, M., Nuccitelli, A., Cozzi, R., Norais, N., Telford, J. L., Rinaudo, C. D., Grandi, G., and Maione, D. (2011) Sortase A substrate specificity in GBS pilus 2a cell wall anchoring. *PLoS One* **6**, e25300
18. Robert, X., and Gouet, P. (2014) Deciphering key features in protein structures with the new ENDscript server. *Nucleic Acids Res.* **42**, W320–W324
19. Klock, H. E., and Lesley, S. A. (2009) The polymerase incomplete primer extension (PIPE) method applied to high-throughput cloning and site-directed mutagenesis. *Methods Mol. Biol.* **498**, 91–103
20. Kabsch, W. (2010) Xds. *Acta Crystallogr. D Biol. Crystallogr.* **66**, 125–132
21. Collaborative Computational Project, Number 4. (1994) The CCP4 suite: programs for protein crystallography. *Acta Crystallogr. D Biol. Crystallogr.* **50**, 760–763
22. Vagin, A., and Teplyakov, A. (1997) MOLREP: an automated program for molecular replacement. *J. Appl. Cryst.* **30**, 1022–1025
23. Adams, P. D., Afonine, P. V., Bunkóczi, G., Chen, V. B., Davis, I. W., Echols, N., Headd, J. J., Hung, L. W., Kapral, G. J., Grosse-Kunstleve, R. W., McCoy, A. J., Moriarty, N. W., Oeffner, R., Read, R. J., Richardson, D. C., Richardson, J. S., Terwilliger, T. C., and Zwart, P. H. (2010) PHENIX: a comprehensive Python-based system for macromolecular structure solution. *Acta Crystallogr. D Biol. Crystallogr.* **66**, 213–221
24. Emsley, P., Lohkamp, B., Scott, W. G., and Cowtan, K. (2010) Features and development of Coot. *Acta Crystallogr. D Biol. Crystallogr.* **66**, 486–501
25. Chen, V. B., Arendall III, W. B., Headd, J. J., Keedy, D. A., Immormino, R. M., Kapral, G. J., Murray, L. W., Richardson, J., J., and Richardson, D. C. (2009) MolProbity: all-atom structure validation for macromolecular crystallography. *Acta. Crystallogr. D Biol. Crystallogr.* **66**, 12–21
26. Banci, L., Bertini, I., Durazo, A., Girotto, S., Gralla, E. B., Martinelli, M., Valentine, J. S., Vieru, M., and Whitelegge, J. P. (2007) Metal-free superoxide dismutase forms soluble oligomers under physiological conditions: a possible general mechanism for familial ALS. *Proc. Natl. Acad. Sci. USA* **104**, 11263–11267
27. Holm, L., and Rosenström, P. (2010) Dali server: conservation mapping in 3D. *Nucleic Acids Res.* **38**, W545–W549
28. Manzano, C., Izoré, T., Job, V., Di Guilmi, A. M., and Dessen, A. (2009) Sortase activity is controlled by a flexible lid in the pilus biogenesis mechanism of gram-positive pathogens. *Biochemistry* **48**, 10549–10557
29. Swaminathan, A., Mandlik, A., Swierczynski, A., Gaspar, A., Das, A., and Ton-That, H. (2007) Housekeeping sortase facilitates the cell wall anchoring of pilus polymers in *Corynebacterium diphtheriae*. *Mol. Microbiol.* **66**, 961–974
30. Barnett, T. C., Patel, A. R., and Scott, J. R. (2004) A novel sortase, SrtC2, from *Streptococcus pyogenes* anchors a surface protein containing a QVPTGV motif to the cell wall. *J. Bacteriol.* **186**, 5865–5875
31. Marraffini, L. A., and Schneewind, O. (2007) Sortase C-mediated anchoring of BasI to the cell wall envelope of Bacillus anthracis. *J. Bacteriol.* **189**, 6425–6436
32. Cozzi, R., Malito, E., Nuccitelli, A., D'Onofrio, M., Martinelli, M., Ferlenghi, I., Grandi, G., Telford, J. L., Maione, D., and Rinaudo, C. D. (2011) Structure analysis and site-directed mutagenesis of defined key residues and motives for pilus-related sortase C1 in group B *Streptococcus*. *FASEB J.* **25**, 1874–1886
33. Neiers, F., Madhurantakam, C., Fälker, S., Manzano, C., Dessen, A., Normark, S., Henriques-Normark, B., and Achour, A. (2009) Two crystal structures of pneumococcal pilus sortase C provide novel insights into catalysis and substrate specificity. *J. Mol. Biol.* **393**, 704–716
34. Manzano, C., Contreras-Martel, C., El Mortaji, L., Izore, T., Fenel, D., Vernet, T., Schoehn, G., Di Guilmi, A. M., and Dessen, A. (2008) Sortase-mediated pilus fiber biogenesis in *Streptococcus pneumoniae*. *Structure* **16**, 1838–1848
35. Khare, B., Fu, Z. Q., Huang, I. H., Ton-That, H., and Narayana, S. V. (2011) The crystal structure analysis of group B *Streptococcus* sortase C1: a model for the "lid" movement upon substrate binding. *J. Mol. Biol.* **414**, 563–577
36. Cozzi, R., Prigozhin, D., Rosini, R., Abate, F., Bottomley, M. J., Grandi, G., Telford, J. L., Rinaudo, C. D., Maione, D., and Alber, T. (2012) Structural basis for group B streptococcus pilus 1 sortases C regulation and specificity. *PLoS One* **7**, e49048
37. Cozzi, R., Zerbini, F., Assfalg, M., D'Onofrio, M., Biagini, M., Martinelli, M., Nuccitelli, A., Norais, N., Telford, J. L., Maione, D., and Rinaudo, C. D. (2013) Group B *Streptococcus* pilus sortase regulation: a single mutation in the lid region induces pilin protein polymerization *in vitro*. *FASEB J.* **27**, 3144–3154
38. Lu, G., Qi, J., Gao, F., Yan, J., Tang, J., and Gao, G. F. (2011) A novel "open-form" structure of sortaseC from *Streptococcus suis*. *Proteins* **79**, 2764–2769
39. Stamnaes, J., Pinkas, D. M., Fleckenstein, B., Khosla, C., and Sollid, L. M. (2010) Redox regulation of transglutaminase 2 activity. *J. Biol. Chem.* **285**, 25402–25409
40. Levin, L., Zelzion, E., Nachliel, E., Gutman, M., Tsfadia, Y., and Einav, Y. (2013) A single disulfide bond disruption in the β3 integrin subunit promotes thiol/disulfide exchange, a molecular dynamics study. *PLoS One* **8**, e59175
41. Chaiswing, L., and Oberley, T. D. (2010) Extracellular/microenvironmental redox state. *Antioxid. Redox Signal.* **13**, 449–465
42. Zähner, D., and Scott, J. R. (2008) SipA is required for pilus formation in *Streptococcus pyogenes* serotype M3. *J. Bacteriol.* **190**, 527–535
43. Mishra, A., Das, A., Cisar, J. O., and Ton-That, H. (2007) Sortase-catalyzed assembly of distinct heteromeric fimbriae in *Actinomyces naeslundii*. *J. Bacteriol.* **189**, 3156–3165
44. Bagnoli, F., Moschioni, M., Donati, C., Dimitrovska, V., Ferlenghi, I., Facciotti, C., Muzzi, A., Giusti, F., Emolo, C., Sinisi, A., Hilleringmann, M., Pansegrau, W., Censini, S., Rappuoli, R., Covacci, A., Masignani, V., and Barocchi, M. A. (2008) A second pilus type in *Streptococcus pneumoniae* is prevalent in emerging serotypes and mediates adhesion to host cells. *J. Bacteriol.* **190**, 5480–5492
45. Okura, M., Osaki, M., Fittipaldi, N., Gottschalk, M., Sekizaki, T., and Takamatsu, D. (2011) The minor pilin subunit Sgp2 is necessary for assembly of the pilus encoded by the srtG cluster of *Streptococcus suis*. *J. Bacteriol.* **193**, 822–831

Received for publication April 27, 2015.
Accepted for publication July 13, 2015.